Inorganica Chimica Acta, 198–200 (1992) 771–780

Synthesis and molecular structure of optically active oxazolidine complexes of platinum(II) and palladium(II)

A. Albinati, F. Lianza
Istituto di Chimica Farmaceutica, Università di Milano, I-20131 Milan (Italy)

H. Berger, C. Arz and P. S. Pregosin*
Laboratorium für anorganische Chemie, ETH Zentrum CH-8092, Zurich (Switzerland)

Abstract

Two series of optically active complexes of the type *trans*-$PtCl_2(C_2H_4)$(oxazolidine) (**3**) and *trans*-$PdCl_2(PPh_3)$(oxazolidine) (**4**), oxazolidine = $\overline{\mathrm{NHCH}(p\text{-}\mathrm{ClC_6H_4})\mathrm{OCH_2C}}\mathrm{HR}$ (R = **a**, Me; **b**, Et; **c**, Bu^i; **d**, Bz; **e**, Ph) have been prepared and characterized. The synthesis involves metal promoted cyclization of the optically active Schiff's bases p-$ClC_6H_4CH{=}NCH(R)CH_2OH$ and proceeds for both metal centers in high chemical and optical yield (diastereomeric excesses of 78–96%). Attack of the oxygen at the imine carbon results in preferential formation of complexed five-membered rings which have the *cis*-geometry with respect to the C-2 and C-5 substituents. The solid-state structures for **3b** and **4c** have been determined by X-ray diffraction. Both structures reveal expected coordination spheres with the MCl_2 (C_2H_4 or PPh_3) fragment occupying a pseudo *trans* position with respect to the oxazolidine C-2, C-5 substituents. This observation, combined with solution 2-D NOESY measurements, is used to rationalize the observed diastereomeric excesses. Crystallographic data for the complexes are as follows: **3b**, orthorhombic, space group $P2_12_12_1$, $a = 7.003(1)$, $b = 16.573(1)$, $c = 29.088(4)$ Å, $V = 3376.1(7)$ Å^3, $Z = 8$; **4c**, orthorhombic space group $P2_12_12_1$, $a = 11.921(2)$, $b = 12.241(1)$, $c = 21.107(2)$ Å, $V = 3080(1)$ Å^3, $Z = 4$. The structures have been refined to R factors of 0.04 and 0.05, respectively.

Introduction

Transition metal complexes are rapidly becoming useful synthetic tools in organic synthesis [1]. This is partly related to their ability to coordinate organic compounds with a consequent change in electrophilicity or nucleophilicity of the coordinated material. The result of this transformation is often an organic fragment with increased reactivity and/or selectivity relative to an uncomplexed organic analog. In connection with our studies on aldimine complexes we have observed that the carbon of a CH=N– function can be more susceptible to attack by alcohols when the electronic structure of the imine has been effected by either direct coordination of the imine nitrogen, or coordination of a functionality in close proximity to the imine [2].

Our interest has settled on α-aminoethers and, specifically on the cyclic derivatives **1**. These are representatives of a well known group of compounds whose relative stabilities are related to the individual structures, e.g. R'' = acyl or alkyl is more stable than $R'' = H$. It has been shown that aminoethers related to **1** are useful synthetic intermediates [3] and an increasing number of reports concern themselves with the use of chiral analogs of **1** as auxiliaries. For $R'' = H$, the compounds **1** can arise from the intramolecular attack of the OH function of **2** on the imine carbon.

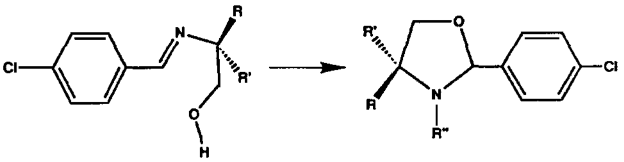

2 **1**

Indeed, in $CDCl_3$ solution, we observe an equilibrium associated with the transformation of **1** into **2**, with the value of K depending on both structure and solvent. As we expected the electrophilicity of the imine carbon to increase on coordination of the nitrogen, we have studied the above cyclization in the presence of $K[PtCl_3(C_2H_4)]$, or the halogen bridged dimer $[PdCl_2(PPh_3)]_2$, both of which are expected to readily coordinate a secondary nitrogen ligand. We report here the synthesis and characterization of two series of surprisingly stable oxazolidine complexes, **3** and **4**, which result from the cyclization of some optically active Schiff's bases, as well as the solid-state structures of two representative complexes. In an earlier commu-

---

*Author to whom correspondence should be addressed.

0020-1693/92/$5.00 © 1992 – Elsevier Sequoia. All rights reserved

nication [4] we described the solid-state structure for a six-membered ring analog together with some preliminary results for **3** and **4**.

Results and discussion

In Scheme 1 we show the transformation of the benzylidene amines, **2**, into the Pt(II) and Pd(II) coordinated oxazolidines, **3** and **4**, respectively. Although most of this study concerns itself with *p*-Cl compounds, we have also carried out some reactions using aromatic nitro-analogs with qualitatively the same results.The isolated yields are good-to-excellent and if the aminoalcohol used to prepare the Schiff's base products is optically pure, the corresponding oxazolidines are optically active. We will return to this subject. Somewhat surprisingly, the products **3** and **4** are relatively resistant to hydrolysis in modestly wet organic solvents. In the hope of finding a simple structural source for this relative stability, we have determined one solid-state structure for each of our complex type.

Molecular structures for 3b and 4c

The molecular structures for **3b** and **4c** were determined by X-ray diffraction and ORTEP views of these molecules are shown in Figs. 1 and 2. Tables 1 and 2 show selected bond lengths and bond angles for these molecules and Table 3 contains literature data from a selection of platinum and palladium complexes for comparison purposes.

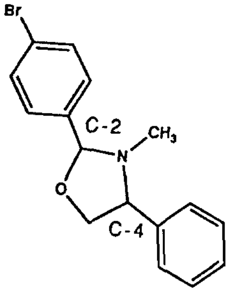

5

Both **3b** and **4c** show distorted square planar coordination at the metal centers and have *trans* geometry with respect to the orientation of the two halogens. The average M–Cl bond separations at 2.285(3) and 2.286(3) Å are as expected [15]. The Pt–N separation, 2.10(1) Å, is in the middle of the literature range, whereas the Pd–N separation, 2.166(8) Å, is on the upper end of the expected range. This difference is doubtless related to the larger *trans* influence of a PPh$_3$ relative to that for ethylene [16] and a comparison of some of the data shown in Table 3 makes this point obvious. Since the heterocyclic nitrogen ligand has only a moderate *trans* influence [16], the Pt–C (olefin) and Pd–P bond distances are relatively short. If we accept

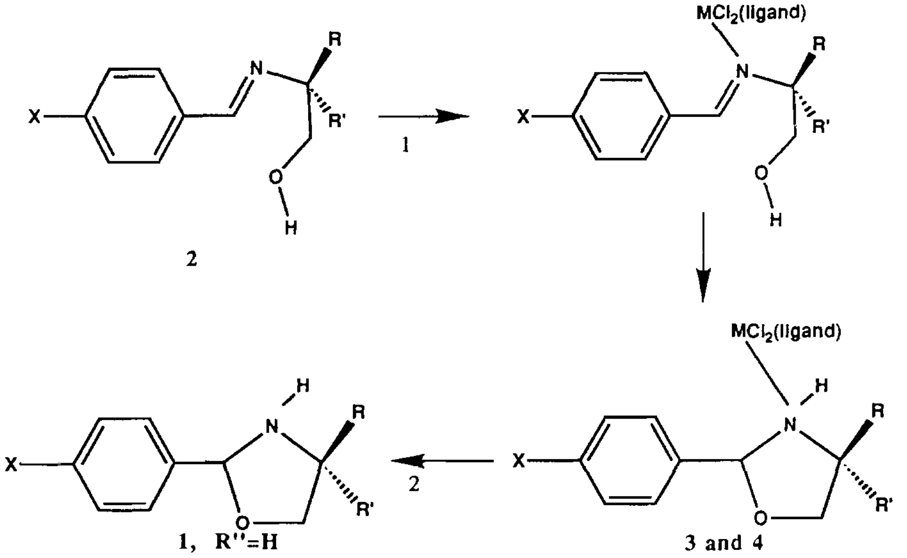

3	M = platinum, ligand = ethylene	**4**	M = palladium, ligand = PPh$_3$
3a	R' = Me	**4a**	R = Me
3b	R' = Et	**4b**	R' = Et
3c	R' = Bu^i	**4c**	R' = Bu^i
3d	R' = Bz	**4d**	R' = Bz
4e	R' = Ph	**4f**	R' = Ph

Scheme 1. M = Pt, ligand = ethylene; M = Pd, ligand = PPh$_3$. 1 = reaction with Zeise's salt or reaction with [PdCl$_2$(PPh$_3$)]$_2$; 2 = reaction with PPh$_3$: 2 equiv. with the ethylene Pt complex, 1 equiv. with the Pd PPh$_3$ complex. For the R(+) enantiomer R = H; R' = **a**, Et; **b**, benzyl; **c**, Me; **d**, Ph; **d**, Bu^i.

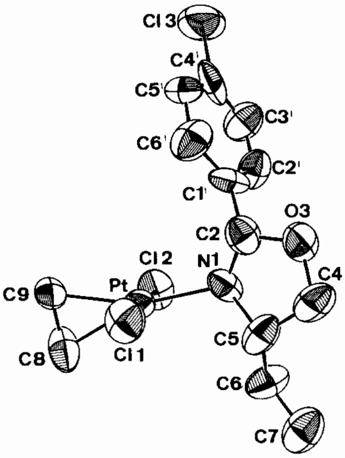

Fig. 1. ORTEP plot of **3b**.

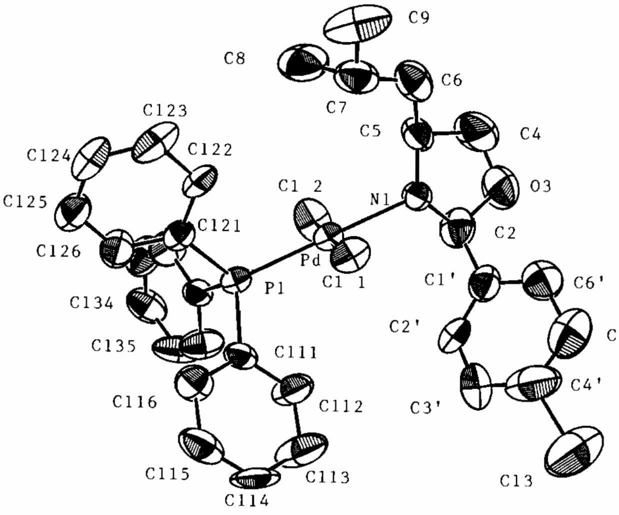

Fig. 2. ORTEP plot of **4c**.

TABLE 1. Bond lengths (Å) and bond angles (°) for **3b**

	Molecule 1	Molecule 2
Pt–Cl(1)	2.283(5)	2.287(6)
Pt–Cl(2)	2.281(6)	2.288(6)
Pt–N(1)	2.10(1)	2.10(1)
Pt–C(8)	2.16(2)	2.15(2)
Pt–C(9)	2.17(2)	2.21(2)
N(1)–C(2)	1.47(2)	1.47(2)
N(1)–C(5)	1.54(2)	1.52(2)
C(2)–O(3)	1.36(2)	1.39(2)
O(3)–C(4)	1.45(2)	1.44(3)
C(4)–C(5)	1.50(3)	1.49(3)
C(2)–C(1′)	1.48(2)	1.54(3)
Cl(1)–Pt–Cl(1′)	177.6(2)	177.3(2)
N(1)–Pt–C(mid)[a]	178.4(10)	178.2(11)
N(1)–Pt–Cl(1)	87.2(4)	85.9(4)
N(1)–Pt–Cl(2)	90.6(2)	91.6(4)
C(2)–N(1)–C(5)	105.4(14)	102.8(13)
N(1)–C(5)–C(4)	99.1(16)	101.3(15)
C(5)–C(4)–O(3)	108.5(17)	107.3(17)
C(4)–O(3)–C(2)	109.9(15)	108.5(15)
N(1)–C(2)–O(3)	104.7(15)	103.8(14)

[a] Mid-point of C–C bond in ethylene.

TABLE 2. Bond lengths (Å) and bond angles (°) for **4c**

Pd–Cl(1)	2.292(3)
Pd–Cl(2)	2.280(3)
Pd–N(1)	2.166(8)
Pd–P(1)	2.255(3)
N(1)–C(2)	1.46(1)
N(1)–C(5)	1.49(1)
C(2)–O(3)	1.40(1)
O(3)–C(4)	1.38(2)
C(4)–C(5)	1.54(2)
C(2)–C(1′)	1.50(2)
C(5)–C(6)	1.54(2)
Cl(1)–Pd–Cl(2)	177.4(1)
N(1)–Pd–P(1)	177.6(6)
N(1)–Pd–Cl(1)	87.5(3)
N(1)–Pd–Cl(2)	90.2(3)
P(1)–Pd–Cl(1)	90.1(1)
P(1)–Pd–Cl(2)	92.2(1)
C(2)–N(1)–C(5)	103.0(8)
N(1)–C(5)–C(4)	103.8(9)
C(5)–C(4)–O(3)	106.6(11)
C(4)–O(3)–C(2)	109.5(9)
O(3)–C(2)–N(1)	107.1(10)

data from the X-ray structure [17] for **5** (for which a slightly different numbering system was used) as representative of an uncoordinated oxazolidine, then we note that there are no significant differences in the C(2)–N or C(2)–O bond distances between **5** and our two complexes.

Although the oxazolidines are moderate in size they do not induce significant distortions in terms of the coordination angles. The Cl–M–Cl angles at 177.5(2) and 177.4(1)° for the Pt and Pd structures, respectively, are normal. The average Cl–M–N angles are 86.6(9) and 91.1(7)° in the Pt complex and 87.5(3) and 90.2(3)° in the Pd complex, thereby completing coordination spheres for these molecules in which all of the ligands occupy their routine places for square planar geometry. The planes defined by the five atoms of the heterocycle in **3b** and **4c** make angles of 87 and 96°, respectively, with the coordination planes of the Pt and Pd complexes. We note that the C(2) and C(5) substituents are *cis* as has been found previously in the solid-state structures [17, 18] of uncomplexed oxazolidines, e.g. for **5**. The *p*-Cl aryl plane is twisted away from the heterocycle plane in both complexes (73 and 81° for the two molecules of **3b**, 56° in **4c**). The five-membered rings are puckered in both compounds.

An important feature of both structures concerns the *cis* relation of the substituents at C-2 and C-5. As we shall show, this structural feature is associated with

TABLE 3. M–N and M–P bond lengths (Å) and *trans* influence

Complex	M–N	M–P	Reference
trans-PtCl$_2$(pyridine)$_2$	1.98(1)		5
cis-PtCl$_2$(pyridine)$_2$	2.01(1), 2.04(1)		5
3b	2.10(1)		this work
trans-PtCl$_2$(DMSO)(pyridine)	2.052(6)		6
PtCl(Me$_2$NCH$_2$CH$_2$NMe$_2$)(C$_2$H$_4$)$^{y+}$	2.084(2)[a] 2.119(2)[b]		7
trans-PtCl$_2$(p-NO$_2$C$_6$H$_4$CHNHCH$_2$CH$_2$O)(C$_2$H$_4$)	2.107(6)		
{*trans*-PtCl$_2$(PEt$_3$)}$_3$(1,3,5-triazine)	2.15(1)	2.219(5)	8
trans-PtCl$_2$(quinoline-8-carboxaldehyde)(PEt$_3$)	2.160(2)	2.222(4)	9
4c	2.166(8)	2.250(3)	this work
cis-PdCl$_2$(PMe$_2$Ph)$_2$		2.260(2)	10
trans-PdCl$_2$(2-NH$_2$,3-CH$_3$-pyridine)(PEt$_3$)	2.155(5)	2.228(2)	11
trans-PdCl$_2$(PPh$_3$)$_2$		2.337(1)	12
trans-PdCl$_2$(oxazole)$_2$	2.016(2)		13
trans-PdCl$_2$(2-methylindole)$_2$	2.024(7)		14

[a] *trans* to Cl. [b] *trans* to C$_2$H$_4$.

TABLE 4. ^{1}H NMR data for the Schiff's bases

	R–Et	S–Et	S–Me	S–Bu^i
H–C(1)	d, 3.738	d, 3.737	m, 3.68	m, 3.68
H–C(2)	m, 3.17	m, 3.19	m, 3.49	m, 3.40
H–C(3)	m, 1.6	m, 1.61	d, 1.18	m, 1.52
H–C(4)	t, 0.853	t, 0.84		m, 1.33
H–C(5)				m, 0.88
H–C(6)				m, 0.88
H–C(7′)	s, 8.18	s, 8.20	s, 8.22	s, 8.23
H–C(2′,6′)	m, 7.61	m, 7.62	m, 7.60	m, 7.64
H–C(3′,5′)	m, 7.346	m, 7.35	m, 7.34	m, 7.365
H–O	s, 2.44	s, 2.34	s, 2.61	s, 2.20

	S–Bz	S–Ph
H–C(1)	m, 3.83	m, 3.94
H–C(2)	m, 3.54	m, 4.48
H–C(3)	m, 2.90	
H–Ar	m, 7.1–7.43	m, 7.24–7.59
H–C(7′)	s, 7.86	s, 8.29
H–C(2′,6′)	m, 7.55	m, 7.67
H–C(3′,5′)	m, 7.33	m, 7.24–7.59
H–O	s, 2.75	s, 2.80

TABLE 5. ^{1}H NMR for the cyclized form of the ligands

	R–Et	S–Et	S–Me	S–Bu^i
H–C(2)	s, 5.39	s, 5.39	s, 5.40	s, 5.39
	s, 5.48	s, 5.49	s, 5.55	s, 5.53
H–C(4)	m, 3.37	m, 3.37	m, 3.30	m, 3.35
H–C(5)	m, 4.02	m, 4.02	m, 4.04	m, 4.04
H–C(1″)	m, 1.6	m, 1.61	m, 1.25	m, 1.52
H–C(2″)	m, 0.98	m, 1.00		m, 1.33
H–C(3″)				m, 0.935
H–C(4″)				
				m, 0.935
H–C(2′,3′,5′,6′)	m, 7.346	m, 7.35	m, 7.34	m, 7.365
H–N	[a]	[a]	[a]	[a]

	S–Bz	S–Ph
H–C(2)	s, 5.43	s, 5.56
	s, 5.57	s, 5.66
H–C(4)	m, 3.83	m, 3.94
H–C(5)	m, 3.96	m, 4.33
H–C(1″)	m, 2.90	–
H–Ar	m, 7.1–7.43	m, 7.24–7.59
H–C(2′,3′,5′,6′)	m, 7.1–7.43	m, 7.24–7.59
H–N	[a]	[a]

[a] Covered by the O–H signal.

the major isomer in solution. The relative position of the metal and ligands with respect to these substituents is best described as pseudo-*trans*. Specifically, the C-2 and C-5 groups lie *c.* 0.4–0.8 Å away from one side of the heterocyclic plane whereas the metal lies *c.* 0.4–0.8 Å away from this plane, but in the opposite direction. These structural features have a possible bearing with respect to the enantiomeric excess observed in solution and could not be obtained from the solution studies using NOESY methods. We shall return to this point shortly. In summary: the angles and distances are normal for such complexes and we can find no obvious structural reason for an increased resistance to hydrolysis relative to the uncomplexed ligands. We have recently reported [4] the X-ray structure for *trans*-PtCl$_2$(ethylene)(p-NO$_2$C$_6$H$_4\overline{\mathrm{CHNHCH_2CH_2O}}$), a compound containing a complexed six-membered oxazolidine ring, and find, in that molecule as well, no structural evidence for resistance to hydrolysis.

Solution structures and NMR spectroscopy

The ligands and complexes have all been identified using microanalytical, IR and, primarily, NMR methods. The Schiff's bases all show a typical imine proton at

TABLE 6. ^{13}C NMR data for the Schiff's bases

	R–Et	S–Et	S–Me	S–Bu^i
C(1)	66.10	65.96	67.19	66.34
C(2)	74.68	74.60	67.70	70.89
C(3)	25.04	24.91	18.26	40.82
C(4)	10.8	10.68		21.70
C(5,6)				23.45
				24.37
C(7′)	160.73	160.62	160.25	160.46
C(1′)	136.80	136.67	136.69	136.70
C(2′,6′)	129.59	129.48	129.47	129.49
C(3′,5′)	128.91	128.78	128.78	128.81
C(4′)	134.30	134.16	134.20	134.21
	S–Bz	S–Ph		
C(1)	65.87	67.68		
C(2)	74.29	76.59		
	60.49	72.54		
C(3)	38.97			
C(7′)	161.17	161.53		
C–Ar	126.29	127.38		
	128.32	127.68		
	129.46	128.84		
	129.71	128.9		
	134.16	134.31		
	136.80	137.02		
	138.41	140.47		

TABLE 7. ^{13}C NMR data for the cyclized form of the ligands

	R–Et	S–Et	S–Me	S–Bu^i
C(2)	91.06	90.93	90.874	90.86
	92.34	92.22	92.34	92.13
C(4)	69.07	70.89	72.46	71.39
	71.29	71.17	72.58	71.68
C(5)	59.38	59.28	52.79	55.84
	61.39	61.26	55.11	58.14
C(1″)	26.27	26.15	17.39	42.42
	26.88	26.75		42.79
C(2″)	11.49	11.37		26.30
C(3″,4″)				22.71
				22.88
C(2′,6′)	127.54	128.40	128.41	128.39
	127.69	128.55	128.58	128.57
C(3′,5′)	128.52	127.42	127.37	127.45
	128.67	127.56	127.53	127.59
C(4′)				
	S–Bz	S–Ph		
C(2)	91.05	91.90		
	92.21	92.62		
C(4)	70.60	62.92		
C(5)	58.82	72.18		
C(1″)	39.27			

TABLE 8. ^1H NMR data for **3**

	R–Et	S–Et	S–Me	S–Bu^i
H–C(2)	d, 5.84	d, 5.84	d, 5.88	d, 5.82
J(H–NH) (Hz)	10.28	10.32	10.36	10.41
H–C(4)	m, 3.95	m, 3.92	m, 3.80	m, 3.85
	m, 4.26	m, 4.25	m, 4.30	m, 4.29
H–C(5)	m, 4.08	m, 4.10	m, 4.21	m, 4.18
H–C(1′)	m, 1.77	m, 1.77	d, 1.59	m, 1.49
	m, 2.16	m, 2.15		m, 2.04
H–C(2′)	t, 1.17	t, 1.16		
H–C(3′,4′)				d, 1.02
				d, 1.09
H–C(2″,6″)	m, 7.45	m, 7.44	m, 7.45	m, 7.44
H–C(3″,5″)	m, 7.72	m, 7.71	m, 7.72	m, 7.71
CH_2CH_2	s, 4.696	s, 4.70	s, 4.71	s, 4.68
J(Pt–H) (Hz)	61.7	62.12	61.71	59.41
	S–Bz	S–Ph		
H–C(2)	d, 5.82	d, 5.98		
	10.15 Hz	10.12 Hz		
H–C(4)	m, 4.00	m, 4.39		
	m, 4.20	m, 4.54		
H–C(5)	m, 4.80	m, 5.25		
H–C(1′)	m, 3.02			
	m, 3.33			
H–Ar	m, 7.2–7.4	m, 7.26–7.59		
H–C(2″,6″)	m, 7.60	m, 7.79		
H–C(3″,5″)	m, 7.41			
H–N		m, 5.06		
CH_2CH_2	s, 4.56	s, 4.65		
J(Pt–H) (Hz)	62.4	62.45		

TABLE 9. ^{13}C NMR data for **3**

	R–Et	S–Et	S–Me	S–Bu^i
C(2)	92.85	92.85	92.72	92.83
C(4)	70.83	70.82	72.52	71.73
C(5)	63.36	63.37	58.09	60.71
C(1′)	25.40	25.40	17.54	26.19
C(2′)	10.66	10.66		41.96
C(3′,4′)				22.48
				22.63
C(1″)	136.40	136.38	136.32	136.33
C(4″)	132.17	132.17	132.20	132.17
C(2″,6″)	129.20	129.20	129.15	129.12
C(3″,5′)	128.38	128.39	128.32	128.41
CH_2CH_2	75.21	75.21	76.40	74.93

δ *c.* 8.2, whereas the complexed oxazolidines have the corresponding methine signal at δ *c.* 3.9–5.3. Interestingly, in **3** and **4** this proton is spin–spin coupled to the NH proton so that it appears as a doublet. The platinum compounds show the expected four proton C_2H_4 multiplet with ^{195}Pt satellites (it is worth noting that this signal is not a singlet, but rather appears as an AA′BB′ spin system) whereas the palladium derivatives show a single ^{31}P resonance due to the coordinated PPh_3. The ^1H NMR characteristics for the coordinated oxazolidines are moderately complicated

TABLE 10. ^1H NMR data for **4**

	S–Et	S–Me	S–Bu^i
H–C(2)	d, 5.77	d, 5.80	d, 5.75
J(H–NH) (Hz)	11.09	11.14	11.1
H–C(4)	m, 3.73	m, 3.62	m, 3.64
	m, 4.15	m, 4.19	m, 4.16
H–C(5)	m, 3.94	m, 4.05	m, 3.99
H–C(1′)	m, 1.72	d, 1.60	m, 1.45
	m, 2.22		m, 2.04
H–C(2′)	t, 1.24		m, 2.32
H–C(3′,4′)			d, 1.04
			d, 1.15
H–Ar	m, 7.26–7.75	m, 7.26–7.79	m, 7.24–7.74
H–C(2″,6″)	[a]	[a]	[a]
H–C(3″,5″)	[a]	[a]	[a]
H–N	m, 3.57	m, 3.55	m, 3.48
	S–Bz	S–Ph	
H–C(2)	d, 5.79	d, 5.92	
J(H–NH) (Hz)	10.98	11.03	
H–C(4)	m, 3.80	m, 4.18	
	m, 4.02	m, 4.42	
H–C(5)	m, 4.35	m, 5.16	
H–C(1′)	m, 2.90		
	m, 3.67		
H–Ar	m, 7.20–7.71	m, 7.26–7.85	
H–C(2″,6″)	[a]	[a]	
H–C(3″,5″)	[a]	[a]	
H–N	m, 3.74	4.04	

[a] Overlaps with PPh_3.

TABLE 11. ^{13}C NMR data for **4**

	S–Et	S–Me	S–Bu^i
C(2)	91.76	91.64	91.72
C(4)	70.84	66.32	71.70
C(5)	61.45	56.07	58.68
C(1′)	25.48	11.48	26.52
C(2′)	11.24		41.92
C(3′,4′)			22.78
			23.03
	S–Bz	S–Ph	
C(2)	91.75	92.34	
C(4)	70.59	72.04	
C(5)	60.74	63.60	
C(1′)	38.23		

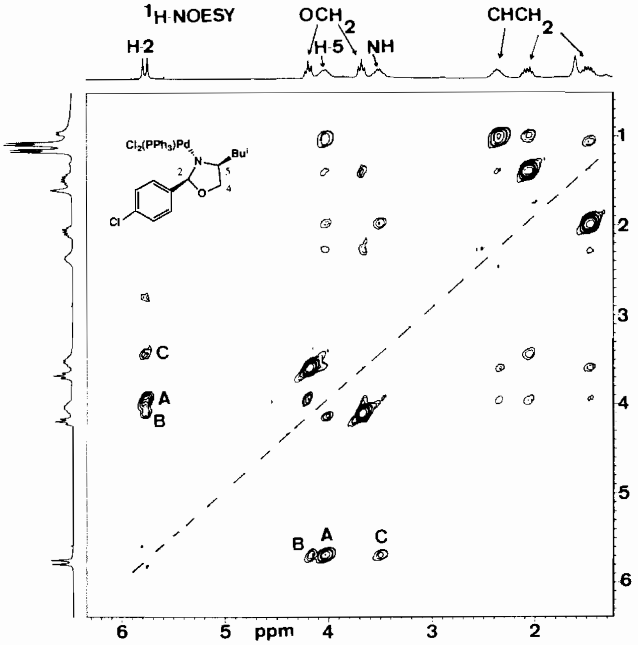

Fig. 3. ^1H phase-sensitive NOESY for complex **4c** ($CDCl_3$, AM-250). The dotted line has been drawn to indicate where the diagonal would be if both phases were plotted. Cross-peak A arises from NOE between H-2 and H-5, whereas cross-peak C develops from the H-2, NH interaction. We have chosen to note cross-peak B, which comes from the interaction of H-2 with one of the two OCH_2 protons. This is useful in that, taken together with the NOE due to one proton of the isobutyl CH_2 and the other OCH_2 proton, this represents an alternative method of determining the C-2, C-5 geometry.

due, in some cases, to the presence of mixtures of diastereomers as well as to the nature of these materials, e.g. the methylene protons are never equivalent. Nevertheless, complete assignment of the important protons in the major diastereomer was always possible using a mixture of one-and two-dimensional NMR methods and summaries of the ^1H and ^{13}C results are shown in Tables 4–11. Based on the values ^2J (Pt, H) and the ^{13}C chemical shift for the coordinated C_2H_4, our oxazolidines exert a moderate *trans* influence similar to that for Cl^- and other nitrogen ligands.

One of the more interesting features of this chemistry concerns the 78–96% diastereomeric excesses observed when the optically active Schiff's bases, **2**, cyclize to form the complexes, **3** and **4** (see Table 2). We have determined the diasteromeric excesses using the ^1H integrals of the methine H-2 and the relative stereochemistry at the C-2 and C-5 carbons using ^1H two-dimensional NOESY methods, as shown in Fig. 3. For both the Pt and Pd complexes these two ring substituents in the major isomer are always *cis* to one another. We assume that the minor isomer has the *trans* geometry*. Figure 3 is illustrative in several ways. First, it shows a strong NOE from H-2 to H-5, thereby confirming the *cis* geometry. Second, there is a significant NOE from the NH to H-2. Taken together with the observed ^3J(NH, CH) value of 11.2 Hz for these two spins, and using known literature [19] on the dihedral angle dependence for such a coupling we conclude that the five-membered ring has adopted a conformation in which

---

*We assume this, although it is possible, but unlikely, that the two isomers arise from the possible orientations of the $PtCl_2$ (ligand) fragment with respect to the C-2 and C-5 substituents.

these two protons are *c.* 150° apart. This places the metal with its ligands pseudo *trans* to the C-2 and C-5 groups. Third, since the data have been obtained in the phase-sensitive mode, we can say that there is no or only very slow exchange between the diastereomers in the complexes since we find no appropriate cross-peaks when the other phases are examined [20].

We note that NOE measurements have been successfully used in the past to determine the geometry of uncomplexed oxazolidines containing tertiary nitrogen atoms [21].

What, then, is the driving force for the preferential formation of one diastereomer? It does not seem related to the nature of the substituent at C-5, in that all of our examples afford qualitatively similar diastereomeric excesses. We believe that the answer involves steric interactions between the *cis* chlorides and the C-2, C-5 substituents and is thermodynamic in origin. NMR studies of the uncomplexed Schiff's bases in $CDCl_3$ solution* show that these are in equilibrium with the *two* diastereomeric oxazolidines. Although the imine form dominates, the two diastereomers are present in almost, but not quite, equal quantities. Certainly there is enough of the *trans* isomer to coordinate and we interpret our results to mean that one of the complexed forms, i.e. that with the least steric hindrance, is the most stable. Preferential complexation of one of the diastereomers shifts the imine–oxazolidine equilibrium such that more of this diastereomer develops and the reaction proceeds until such time as the new equilibrium is reached. Removal of the metal and ligands via the addition of the appropriate amount of PPh_3 to form the stable and sparingly soluble $MCl_2(PPh_3)_2$ affords (after filtration) methylene chloride solutions which contain the imine and cyclic forms in equilibrium in their original composition. Consequently, the metal functions as a rather special 'substituent' for the nitrogen, since it is known [22] that N-substituted oxazolidines are more stable than the open imine form and prefer [17, 18, 21] a *cis* geometry with respect to groups at C-2 and C-5. The metal is useful in that it contributes to stabilizing an oxazolidine which under normal circumstances (i) prefers the imine form and (ii) is readily hydrolyzed.

TABLE 12. Yields and further analytical data for the compounds

Compound	Calc. Found C	H	N	Yield (%)	Diastereom. excess (%) (^{31}P chemical shift)
2a	60.76	6.12	7.09		81
	60.85	6.13	7.38		
2b	62.41	6.67	6.62		83
	62.59	6.79	6.57		
2c	65.40	7.18	5.87		62
	65.14	7.58	5.83		
2d	70.20	5.89	5.12		73
	69.77	5.91	5.72		
2e	69.39	5.43	5.39		88
	69.19	5.36	5.37		
3a	29.31	3.28	2.85	86	93
	29.22	3.32	2.92		
3b	30.87	3.59	2.77	98	93
	30.88	3.58	2.56		
3c	33.75	4.15	2.62	92	95
	33.80	3.89	2.77		
3d	33.08	3.55	2.47	96	78
	32.67	3.44	2.38		
3e	36.87	3.28	2.53	88	92
	36.54	3.31	2.43		
4a	52.77	4.27	2.20	78	82 (28.25)
	52.19	4.59	2.25		
4b	53.48	4.49	2.15	95	90 (28.21)
	53.02	4.51	2.15		
4c	54.81	4.90	2.06	77	92 (28.48)
	54.81	4.99	2.08		
4d	57.25	4.38	1.96	91	86 (28.19)
	57.00	4.62	2.04		
4e	56.65	4.18	2.00	93	92 (28.77)
	56.44	4.22	1.99		

TABLE 13. Analytical and spectroscopic data for additional complexes: $2\text{-}NO_2$, $3\text{-}NO_2$ and $4\text{-}NO_2$ analogs of **3b**

	Calc. Found			^{1}H		^{13}C	
				H-5	C_2H_4^{a}	C-5	C_2H_4
$2\text{-}NO_2$	30.24	3.51	5.43	5.99	4.65	92.73	75.37
	30.39	3.62	5.40		(59.0)		(166.0)
$3\text{-}NO_2$	30.24	3.51	5.43	5.98	4.75	92.45	75.56
	30.44	3.60	5.41		(59.2)		(165.0)
$4\text{-}NO_2$	30.24	3.51	5.43	5.96	4.74	92.42	75.71
	30.49	3.70	5.42		(61.1)		(165.8)

^{a}Coupling to Pt given in parentheses.

Experimental

NMR measurements were performed on Bruker AC-200, AM-250 and AM-500 MHz spectrometers in $CDCl_3$ solutions unless otherwise noted. IR measurements were carried out using a Perkin-Elmer 883 spectrometer and microanalyses were determined by the analytical laboratory of the ETH Zurich. Two-dimensional NOESY experiments were performed as described previously [20, 23–25] using a mixing time of 1.5 s.

Unless otherwise noted the complexes were prepared under a nitrogen atmosphere.

The ligands were all prepared in an identical fashion. A typical preparation is shown below; yields and details are given in Table 12.

---

*Interestingly, the 2-D exchange spectrum shows that the diastereomers exchange with the imine but **not** with each other.

TABLE 14. Experimental data for the X-ray diffraction study of **3b** and **4c**

Compound	**3b**	**4c**
Formula	$C_{13}H_{17}Cl_3NOPt$	$C_{13}H_{32}Cl_3NOPd$
Molecular weight	504.724	678.356
Crystal dimensions	0.20×0.25×0.50	0.15×0.25×0.20
Data collection temperature (°C)	r.t.	r.t.
Crystal system	orthorombic	orthorombic
Space group	$P2_12_12_1$	$P2_12_12_1$
a (Å)	7.003(1)	11.921(2)
b (Å)	16.573(1)	12.241(1)
c (Å)	29.088(4)	21.107(8)
V (Å^3)	3376.1(7)	3080.1(1.1)
Z	8	4
ρ_{calc} (g cm^{-3})	1.985	1.462
μ (cm^{-1})	88.66	9.33
Radiation	Mo Kα	(graphite monochromated $\lambda=0.71069$ Å)
Measured reflections	$+h,\ +k,\ +l$	$+h,\ +k,\ +l$
θ range (°)	$2.2<\theta<25.0$	$2.5<\theta<27.0$
Scan type	$\omega/2\theta$	$\omega/2\theta$
Scan width (°)	$1.0+0.35\tan\theta$	$1.1+0.35\tan\theta$
Max. counting time(s)	65	70
Background time (s)	0.5×scan-time	
Max. scan speed (° min^{-1})	6.9	5.2
Prescan rejection limit	0.5 (1.82 σ)	0.5 (1.82 σ)
Prescan acceptance limit	0.025 (40.00 σ)	0.025 (40.00 σ)
Horizontal receiving slit (mm)	$1.80+\tan\theta$	$1.75+\tan\theta$
Vertical receiving slit (mm)	4.0	4.0
Transmission coefficient	0.9956–0.5288	0.9936–0.9155
No. independent data collected	3422	3438
No. observed reflections (n_o) ($\|F_o\|^2>2.5\sigma(\|F\|^2)$)	2085	2191
No. parameters refined (n_v)	343	343
R[a]	0.040	0.049
R_w[b]	0.055	0.062
GOF[c]	1.131	1.289
f	0.080	0.070

[a] $R=\Sigma\|\|F_o\|-1/k\|F_c\|\|/\Sigma\|F_o\|$. [b] $R_w=[\Sigma w(|F_o|-1/k|F_c|)^2/\Sigma w|F_o|^2]^{1/2}$ where $w=[\sigma^2(F_o)]^{-1}$ and $\sigma(F_o)=[\sigma^2(I)+f^2(F_o^2)^2]^{1/2}/2F_o$. [c] $GOF=[\Sigma w(|F_o|-(1/k)|F_c|)^2/(n_o-n_v)]^{1/2}$.

Synthesis of (S)-N-(4'chlorobenzylidene)-2-aminobutane-1-ol

(R)-2-Amino-butane-1-ol (0.671 g, 7.53 mmol) and p-chlorobenzaldehyde (1.058 g, 7.53 mmol) were dissolved in 30 ml toluene. The resulting solution was then warmed to 333 K at c. 200 torr for 3 h in a Dean–Stark trap, in which 1 g of $MgSO_4$ had been placed (to help absorb water). The solvent was removed i.v. and the resulting oil recrystallized from hexane to afford the product as a white solid in 83% yield.

Synthesis of dichloro-ethylene-[(2R, 5R)-2-(4'-chlorophenyl)-5-ethyl-oxazolidine]platinum(II)

The Schiff's base (72 mg, 0.136 mmol) and Zeise's salt (50 mg, 0.136 mmol) were placed in a 25 ml flask. Addition of c. 2–3 ml of previously dried (over basic Alox from Woelm) methylene chloride was followed by stirring the reaction mixture for 2 h. The solution was separated from the KCl using a pipette and the solvent subsequently removed i.v. Recrystallization from methylene/hexane, 1:10, afforded the product as a yellow solid in 96% yield. This procedure was used to prepare several analogs with nitro substituents in the 2,3 and 4 positions of the aryl ring at C-2. We show selected data for these complexes in Table 13.

The same procedure used for the Pt complexes was employed in the preparation of the palladium compounds, with the following exception: argon was used as inert atmosphere and the suspension was stirred for only 30 min before work-up. The starting material for the palladium reactions was the chloride bridged dimer $[PdCl_2(PPh_3)]_2$. We have also prepared a Pt analog using $PMePh_2$ as phosphine and show selected data for this in Table 13.

Structural studies

*trans-$PtCl_2(C_2H_4)$(oxazolidine) (**3b**)*

A prismatic crystal with elongated habit was mounted on a glass fiber at a random orientation for the unit cell and space group determination and for the data collection. Unit cell dimensions were obtained by least-squares fit of the 2θ values of 25 high order reflections

TABLE 15. Final positional parameters and equivalent temperature factors (Å^2) for **3b** (e.s.d.s are given in parentheses)

Atom	x	y	z	B (Å^2)
Pt1	0.8736(1)	0.65639(4)	0.15603(2)	4.38(1)
Pt1A	0.5136(1)	0.83158(4)	0.65968(3)	4.69(1)
Cl1	1.1192(8)	0.5691(3)	0.1699(2)	6.7(1)
Cl1A	0.2639(9)	0.9167(3)	0.6745(2)	7.2(1)
Cl2	0.6371(7)	0.7478(4)	0.1422(2)	7.1(1)
Cl2A	0.7544(8)	0.7432(4)	0.6426(2)	6.9(1)
Cl3	1.315(2)	0.5260(4)	−0.0580(2)	11.5(3)
Cl3A	0.133(2)	0.9739(4)	0.4443(2)	11.3(3)
O3	1.199(2)	0.8297(7)	0.0836(5)	6.8(4)
O3A	0.196(2)	0.6614(8)	0.5826(5)	7.3(4)
N1	1.080(2)	0.7388(9)	0.1327(5)	5.2(4)
N1A	0.306(2)	0.7513(9)	0.6344(5)	4.4(3)
C1′	1.132(3)	0.702(1)	0.0505(5)	5.1(4)
C1′A	0.282(3)	0.794(1)	0.5521(6)	5.3(5)
C2	1.079(3)	0.765(1)	0.0845(7)	5.8(5)
C2′	1.003(4)	0.676(1)	0.0171(7)	7.3(6)
C2A	0.325(3)	0.725(1)	0.5863(6)	5.2(5)
C2′A	0.091(3)	0.817(1)	0.5470(7)	5.7(5)
C3′	1.069(4)	0.618(1)	−0.0157(6)	8.1(7)
C3′A	0.050(4)	0.876(1)	0.5143(6)	6.8(6)
C4′	1.243(3)	0.596(1)	−0.0160(8)	7.2(5)
C4A	0.185(3)	0.621(1)	0.6265(8)	7.6(6)
C4′A	0.176(4)	0.903(1)	0.4879(6)	6.7(6)
C4	1.203(3)	0.868(1)	0.1284(7)	7.1(6)
C5A	0.291(2)	0.672(1)	0.6602(7)	4.7(4)
C5	1.092(3)	0.817(1)	0.1613(8)	6.4(5)
C5′A	0.354(4)	0.886(2)	0.4923(7)	9.2(7)
C5′	1.365(3)	0.615(1)	0.0177(7)	6.9(6)
C6A	0.197(3)	0.686(1)	0.7092(8)	7.2(6)
C6′A	0.418(4)	0.826(1)	0.5289(8)	8.0(6)
C6′	1.314(3)	0.672(1)	0.0504(7)	5.9(5)
C6	1.180(4)	0.803(1)	0.2100(7)	7.3(6)
C7	1.188(3)	0.881(2)	0.2359(9)	8.3(7)
C7A	0.180(5)	0.603(2)	0.731(1)	10.8(9)
C8A	0.701(3)	0.894(1)	0.7066(6)	7.2(6)
C8	0.687(3)	0.590(1)	0.2014(7)	7.1(6)
C9	0.670(3)	0.558(1)	0.1568(6)	6.0(5)
C9A	0.723(4)	0.931(1)	0.6655(7)	7.5(5)

Anisotropically refined atoms are given in the form of the isotropic equivalent displacement parameter defined as: $(4/3)\ [a^2\beta(1,1)+b^2\beta(2,2)+c^2\beta(3,3)+ab(\cos\gamma)\beta(1,2)+ac(\cos\beta)\beta(1,3)+bc(\cos\alpha)\beta(2,3)]$.

TABLE 16. Final positional parameters and equivalent temperature factors (Å^2) for **4c** (e.s.d.s are given in parentheses)

Atom	x	y	z	B (Å^2)
Pd	0.92842(6)	0.96613(6)	0.85296(4)	3.05(1)
Cl1	0.8919(3)	0.7860(2)	0.8742(2)	4.38(6)
Cl2	0.9632(3)	1.1438(2)	0.8271(2)	5.79(8)
Cl3	0.4856(5)	0.6957(7)	0.6850(3)	14.9(2)
P1	0.8721(2)	1.0119(2)	0.9514(1)	3.11(5)
O3	0.9760(9)	0.9491(8)	0.6522(4)	7.0(2)
N1	0.9811(7)	0.9151(8)	0.7593(4)	3.8(2)
C1′	0.801(1)	0.894(1)	0.7015(6)	4.7(3)
C2	0.911(1)	0.954(1)	0.7072(5)	5.4(3)
C2′	0.713(1)	0.913(1)	0.7392(7)	6.6(3)
C3′	0.617(1)	0.865(2)	0.7361(7)	8.5(5)
C4′	0.612(1)	0.785(2)	0.6935(8)	10.2(6)
C4	1.088(1)	0.963(2)	0.6676(6)	8.5(5)
C5′	0.693(1)	0.754(1)	0.6527(8)	7.8(4)
C5	1.0962(9)	0.9498(9)	0.7399(5)	4.4(3)
C6′	0.794(1)	0.817(1)	0.6571(7)	6.0(3)
C6	1.191(1)	0.869(1)	0.7572(7)	5.8(3)
C7	1.208(1)	0.851(1)	0.8248(7)	6.2(3)
C8	1.294(1)	0.764(2)	0.838(1)	10.1(6)
C9	1.253(1)	0.953(1)	0.8567(8)	8.4(4)
C111	0.7350(8)	0.9604(9)	0.9682(5)	3.5(2)
C112	0.659(1)	0.949(1)	0.9200(6)	5.7(3)
C113	0.550(1)	0.910(1)	0.9282(7)	7.5(4)
C114	0.5192(9)	0.875(1)	0.9887(7)	6.5(4)
C115	0.591(1)	0.888(1)	1.0371(7)	6.3(3)
C116	0.701(1)	0.930(1)	1.0276(6)	4.8(3)
C121	0.9677(8)	0.9719(9)	1.0133(5)	3.3(2)
C122	1.0581(9)	0.9006(9)	0.9971(5)	4.4(2)
C123	1.134(1)	0.866(1)	1.0437(7)	6.0(3)
C124	1.121(1)	0.900(1)	1.1050(6)	6.0(3)
C125	1.034(1)	0.971(1)	1.1195(6)	5.8(3)
C126	0.959(1)	1.003(1)	1.0744(6)	4.8(3)
C131	0.8556(9)	1.1594(9)	0.9662(5)	3.5(2)
C132	0.948(1)	1.2235(8)	0.9807(6)	4.9(3)
C133	0.939(1)	1.328(1)	0.9900(6)	6.1(3)
C134	0.839(1)	1.383(1)	0.9848(7)	5.6(3)
C135	0.747(1)	1.319(1)	0.9670(8)	7.1(4)
C136	0.755(1)	1.214(1)	0.9595(7)	5.3(3)

Anisotropically refined atoms are given in the form of the isotropic equivalent displacement parameter defined as: $(4/3)[a^2\beta(1,1)+b^2\beta(2,2)+c^2\beta(3,3)+ab(\cos\gamma)\beta(1,2)+ac(\cos\beta)\beta(1,3)+bc(\cos\alpha)\beta(2,3)]$.

$(9<\theta<15)$ using the CAD4 centering routines. Selected crystallographic and other relevant experimental data are listed in Table 14.

Three standard reflections were measured every hour and used to check the stability of the crystal and of the experimental conditions; no significant variation was detected. The orientation of the crystal was monitored by measuring three standards every 300 reflections.

Data have also been corrected for adsorption using azimuthal (Ψ) scans of three reflections ($\chi>85.4$; $9.4<\theta<15.8$).

Upon convergence (no parameter shift $>0.2\sigma(p)$) the final Fourier difference map showed no significant feature.

trans-$PdCl_2(PPh_3)$*(oxazolidine)* (**4c**)

Crystals of this compound are stable in air. A polyhedral crystal, mounted on a glass fiber at a random orientation, was used for the unit cell and space group determination and for the data collection. Cell constants were obtained by least-squares fit of the 2θ values of 25 high order reflections $(9.5<\theta<17.3)$. Selected crystallographic and other relevant experimental data are listed in Table 14.

Three standard reflections were measured every hour and used to check the stability of the experimental conditions and the decay of the crystal, while the orientation was monitored by measuring three standards every 300 reflections.

An anisotropic decay correction was applied to the collected intensities (correction factors in the range 1.2189–0.8290) as well as an adsorption correction using azimuthal (Ψ) scans of three reflections ($\chi > 86.7$; $10.0 < \theta < 15.4$).

Upon convergence (no parameter shift $> 0.1\sigma(p)$) the final Fourier difference map showed no significant feature.

Crystallography

Crystals suitable for X-ray diffraction of compounds **3b** and **4c** were obtained in both cases by recrystallization from a methylene-chloride/hexane mixture.

Data were collected, for both compounds, on an Enraf-Nonius CAD4 diffractometer by using the parameters listed in Table 14.

Intensities were measured with variable scan speed to ensure constant statistical precision on the collected intensities. Data were corrected for Lorentz and polarization factors using the MOLEN crystallographic package [26]. The standard deviations on intensities were calculated in terms of statistics alone; an $F_o^2 = 0.0$ was given to those reflections having negative net intensities.

The structures were solved by a combination of Patterson and Fourier methods and refined by full matrix least-squares [26] (the function minimized was $[\Sigma w(F_o - 1/k|F_c|)^2]$). No extinction correction was applied to either data set.

The scattering factors used, corrected for the real and imaginary parts of the anomalous dispersion, were taken from the literature [27]. Anisotropic temperature factors were used for all but the hydrogen atoms. The contribution from the hydrogen atoms in their idealized positions (C–H = 0.95 Å, $B = 8.0$ Å^2) was taken into account but not refined.

The handedness of the crystals was tested by refining (to convergence) both enantiomers and comparing the results by means of Hamilton's test [28]. The coordinates corresponding to the sets giving the significantly lower R_w factors are listed in Tables 15 and 16. All calculations were carried out using MOLEN on a μVAX computer.

Supplementary material

Tables of anisotropic displacement parameters, calculated H positions, extended lists of bond lengths and angles, least-squares planes and observed and calculated structure factors for both structures may be obtained from the authors upon request.

Acknowledgements

We thank the Swiss National Science Foundation, the ETH Zurich and the Italian CNR for financial support and the Johnson Matthey Research Centre, UK, for the loan of precious metals. We also thank Mr A. Boller for experimental assistance.

References

1 D. Seebach, G. Stucky and P. Renaud, *Chimia, 42* (1988) 176; D. Seebach, *Angew. Chem., 102* (1990) 1363.

2 A. Albinati, C. Arz and P. S. Pregosin, *Inorg. Chem., 27* (1988) 2015.

3 Y. Yamamoto, H. Sato and J. Yamada, *Synlett.*, (1991) 339; H. Takahashi, H. Niwa and K. Higashiyama, *Heterocycles, 27* (1988) 2099.

4 A. Albinati, C. Arz and P. S. Pregosin, *J. Organomet. Chem., 371* (1989) C18.

5 P. Colamarino and P. L. Orioli, *J. Chem. Soc., Dalton Trans.*, (1975) 1656.

6 F. Caruso, R. Spagna and L. Zambonelli, *Acta Crystallogr., Sect. B, 36* (1980) 713.

7 G. Gervasio, S. A. Mason and G. Natile, *Inorg. Chem., 25* (1986) 2207.

8 W. Kaufmann, L. M. Venanzi and A. Albinati, *Inorg. Chem., 27* (1988) 1178.

9 A. Albinati, C. G. Anklin, F. Ganazzoli, H. Ruegg and P. S. Pregosin, *Inorg. Chem., 26* (1987) 503.

10 L. I. Martin and R. A. Jacobson, *Inorg. Chem., 10* (1971) 1795.

11 A. Albinati, C. Arz and P. S. Pregosin, *Inorg. Chem., 26* (1987) 508.

12 G. Ferguson, R. McCrindle, A. J. McAlees and M. Parvez, *Acta Crystallogr., Sect. B, 38* (1982) 2679.

13 E. Binamira-Soriaga, M. Lundeen and K. Seff, *J. Cryst. Mol. Struct., 9* (1979) 67.

14 O. Yamauchi, M. Takani, K. Toyoda and H. Masuda, *Inorg. Chem., 29* (1990) 1856.

15 W. L. Steffen and G. J. Palenik, *Inorg. Chem., 15* (1976) 2432.

16 T. Appleton, H. C. Clark and L. E. Manzer, *Coord. Chem. Rev., 10* (1973) 335.

17 H. Takahashi, B. Hsieh and K. Higashiyama, *Chem. Pharm. Bull., 38* (1990) 2429.

18 I. Hoppe, D. Hoppe, R. Herbst-Irmer and E. Egert, *Tetrahedron Lett., 31* (1990) 6859.

19 O. Jardetzky and G. C. K. Roberts, *NMR in Molecular Biology*, Academic Press, London, 1981, p. 159.

20 W. E. Hull, *Two-dimensional NMR Spectroscopy*, VCH, New York, 1987, p. 154.

21 S. Arseniyadis, P. P. Q. Huang, N. Morellet, J. Beloeil and H. Husson, *Heterocycles, 31* (1990) 1789.

22 D. Seebach, R. Imwinkelreid and T. Weber, *Modern Synthetic Methods*, Vol. 4, Springer, Berlin, 1986, p. 125.

23 H. Ruegger, R. W. Kunz, C. J. Ammann and P. S. Pregosin, *Magn. Reson. Chem., 29* (1991) 197.

24 A. Albinati, R. W. Kunz, C. J. Ammann and P. S. Pregosin, *Organometallics, 10* (1991) 1800.

25 C. Ammann, P. S. Pregosin and A. Scrivanti, *Inorg. Chim. Acta, 155* (1989) 217.

26 *MOLEN*, structure determination package, Delft Instruments, Delft, Netherlands, 1990.

27 *International Tables for X-ray Crystallography*, Vol. IV, Kynoch, Birmingham, UK, 1974.

28 W. C. Hamilton, *Acta Crystallogr., 13* (1965) 502.